THE JOURNAL OF BIOLOGICAL CHEMISTRY VOL. 289, NO. 46, pp. 31805–31817, November 14, 2014

The E3 Ubiquitin Ligase MID1 Catalyzes Ubiquitination and Cleavage of Fu

Received for publication, December 6, 2013, and in revised form, October 1, 2014 Published, JBC Papers in Press, October 2, 2014, DOI 10.1074/jbc.M113.541219

Susann Schweiger[‡], Stephanie Dorn[§], Melanie Fuchs[¶], Andrea Köhler[‖], Frank Matthes[§], Eva-Christina Müller[**], Erich Wanker[**], Rainer Schneider[‖], and Sybille Krauß[§1]

*From the [‡]Institute for Human Genetics, Medical School, University of Mainz, 55122 Mainz, Germany, the [§]German Center for Neurodegenerative Diseases, 53127 Bonn, Germany, the [¶]Department of Dermatology, Charité University Hospital, 10117 Berlin, Germany, the [‖]Institute of Biochemistry and Center for Molecular Biosciences Innsbruck, 6020 Innsbruck, Austria, and **Max Delbrück Center for Molecular Medicine, 13125 Berlin-Buch, Germany*

Background: SHH signaling is an important growth-stimulating factor in diverse cancers.
Results: MID1 catalyzes ubiquitination and proteasomal cleavage of Fu.
Conclusion: The MID1-PP2A complex regulates the activity of the SHH effector GLI3 in cancer cell lines by regulating proteasomal cleavage of Fu.
Significance: Understanding the molecular mechanisms underlying tumorigenesis is crucial for developing therapeutic approaches to treat cancers.

SHH (Sonic Hedgehog)-GLI signaling plays an important role during embryogenesis and in tumorigenesis. The survival and growth of several types of cancer depend on autonomously activated SHH-GLI signaling. A protein complex containing the ubiquitin ligase MID1 and protein phosphatase 2A regulates the nuclear localization and transcriptional activity of GLI3, a transcriptional effector molecule of SHH, in cancer cell lines with autonomously activated SHH signaling. However, the exact molecular mechanisms that mediate the interaction between MID1 and GLI3 remained unknown. Here, we show that MID1 catalyzes the ubiquitination and proteasomal cleavage of the GLI3 regulator Fu. Our data suggest that Fu ubiquitination and cleavage is one of the key elements connecting the MID1-PP2A protein complex with GLI3 activity control.

Members of the Hh (Hedgehog) protein family are key mediators of several fundamental processes during embryonic development including growth, body patterning, and tissue morphogenesis (reviewed in Refs. 1 and 2). In response to extracellular stimulation, Hh proteins bind to their receptor Patched (Ptch), a 12-span transmembrane protein. In the absence of Hh ligands, Ptch inhibits Smoothened (Smo), a second transmembrane protein. Hh binding leads to the relief of Smo and the activation of a downstream signaling cascade (3). In *Drosophila*, the cytosolic transduction of the Hh signal involves a microtubule-associated protein complex containing Fu (Fused), the GLI family transcription factor Ci (Cubitus Interruptus), the kinesin-like protein Cos2 (Costal2), and SuFu (Suppressor of Fused) (reviewed in Ref. 4). Upon Hh stimulation, the Fu kinase gets phosphorylated and thereby activated, enabling it to phosphorylate Cos2 at two different positions (5, 6). Phosphorylation of Cos2 leads to the release of the entire protein complex from the microtubules. Ci maturates into a transcriptional activator and translocates into the nucleus, where it stimulates transcription of Hh target genes.

Although Hh signaling seems more complex in mammals, several elements of the Hh pathway are highly conserved throughout species. Three homologues of Hh (SHH (Sonic Hedgehog), DHH (Desert Hedgehog), and IHH (Indian Hedgehog) (7)), two Ptch homologues (PTCH1 (Patched 1) and PTCH2 (Patched 2) (8)), and three Ci homologues (GLI1, GLI2, and GLI3) (9, 10) have been identified in mammalian cells (3, 4). Also, a human orthologue of the Fu kinase (11) has been discovered. However, transduction of Hh signals and in particular the function of the mammalian Fu kinase seem to differ substantially from *Drosophila* and are discussed controversially in the literature. Some studies have suggested that human Fu enhances the activator function of GLI proteins similar to its role in *Drosophila* (11–13). Fu knock-out mice, however, do not display typical SHH deficiency phenotypes. Instead, they develop normally until birth, but fail to thrive within the first week, and develop severe growth retardation and hydrocephalus. They die within the first 3 weeks after birth (14, 15).

These data show that although Fu is dispensable for Hh signaling during embryogenesis, its fundamental function evolves after birth, suggesting two different mechanisms of Hh signal transduction in mammals: one is Fu-dependent and important for the regulation of growth and brain formation after birth, and a second one is Fu-independent and either solely responsible for embryonic Hh signaling or at least able to back up for the Fu-dependent pathway in embryonic tissues.

Likewise, mechanisms leading to the activation of mammalian GLI proteins are much less well understood than in *Drosophila*. As we have shown previously, a protein complex consisting of the microtubule-associated ubiquitin ligase MID1, the α4 protein, and protein phosphatase 2A (PP2A)[2] regulates the nuclear localization and transcriptional activity of one of

[1] To whom correspondence should be addressed: German Center for Neurodegenerative Diseases, University of Bonn/BMZ1, Sigmund-Freud-Str. 25, 53127 Bonn, Germany. Tel.: 49-228-28751113; E-mail: sybille.krauss@dzne.de.

[2] The abbreviation used is: PP2A, protein phosphatase 2A.

the three transcriptional effector molecules of mammalian SHH signaling, GLI3, in cancer cell lines with autonomously activated SHH signaling (16, 17). Via its ubiquitin ligase activity, the RING finger protein MID1 targets PP2A toward ubiquitin-dependent degradation by the proteasome and thereby decreases PP2A activity at the microtubules (18). Furthermore, we found that MID1 activity is fundamental for the maturation of GLI3 into a transcriptional activator. However, the exact molecular mechanisms that mediate the interaction between MID1 and GLI3 remain unknown.

Here we show that in mammalian cells, the kinase domain of Fu is cleaved off upon ubiquitination of Fu leading to the expression of a 90-kDa fragment. We further show that this ubiquitination is mediated through interaction of Fu with the MID1 ubiquitin ligase, which targets Fu toward Lys^{6}, Lys^{48}, and Lys^{63} ubiquitination. Blockage of the proteasome leads to a significant increase in abundance of full-length Fu compared with the 90-kDa fragment. Likewise, knockdown of MID1 leads to a remarkable reduction of the 90-kDa fragment. Together with the observation that knockdown of Fu, as well as inhibition of the proteasome, significantly decreases nuclear GLI3, whereas overexpression of Δkinase Fu increases nuclear localization and activity of GLI3, these data suggest that Fu and its ubiquitination and cleavage are key elements connecting the MID1 protein complex with GLI3 activity control.

EXPERIMENTAL PROCEDURES

Immunofluorescence—For immunofluorescence experiments, HeLa or U373MG cells were plated on coverslips (in 6-well plates) at a density of 1×10^5 cells/well 1 day before transfection. Cells were transfected with the respective plasmids using Polyfect transfection reagent (Qiagen) according to the manufacturer's instructions. Twenty-four hours after transfection, cells were fixed with 3.7% paraformaldehyde in PEM buffer (10× PEM contains 1 M Pipes, 0.05 M EGTA, 0.02 M $MgCl_2$, pH 7.0). The GFP-GLI3 signal distribution in individual cells occurred in three patterns: exclusively nuclear fluorescence, evenly stained throughout the cytosol and nucleus, or predominantly cytosolic fluorescence. 100 transfected cells per coverslip were counted and classified in one of the three groups. Each experiment was repeated in triplicate. The data shown represent means ± S.D. scored per group from three independent experiments of 100 cells each. Statistical significance was evaluated using TTest (two-tailed, homoscedastic) or one-way analysis of variance with post hoc Dunnett's test to accommodate for multiple comparisons.

Transfection and Western Blotting—1×10^5 HeLa cells/well of a 6-well plate were seeded 24 h prior transfection. Transfections with the respective plasmids were performed using Polyfect transfection reagent (Qiagen) according to the manufacturer's instructions. For analysis of total cell lysates 48 h after transfection, cells were lysed in 2× Magic Mix (48% urea, 15 mM Tris-HCl, 8.7% glycerol, 1% SDS, 0.004% bromphenol blue, 143 mM β-mercaptoethanol). Samples were denatured at 95 °C, separated on SDS gels, and blotted on PVDF membranes (Roche).

Knockdown Experiments—Twenty-four hours before transfection, HeLa cells were seeded into 6-well plates at a density of 1×10^5 cells/well. Cells were transfected with 1.3 μg of synthetic siRNA per well using Oligofectamine (Invitrogen) according to the manufacturer's instructions. Sequences of siRNAs are listed in Table 1.

TABLE 1
siRNA sequences

siRNA	Gene targeted	Target sequence (5′-3′)
Fu si2	Fu	AAGGCACACCACTCTATATGTCT
Fu si3	Fu	AAGGTAAAAGTAGTAGATTGGGA
Fu si1	Fu	AAGAGTCTACTGAAGTGACACT
MID1si-2	MID1	TGCCATTGGTCTTGCTTACAA
MID1si-4	MID1	GGATTACAACTTTTAGGAATT

TABLE 2
Primer sequences

Primer name (real time PCR)	Target gene	Sequence (5′-3′)
GAPDH-f1	GAPDH	CCACCCATGGCAAATTCC
GAPDH-r1	GAPDH	TGGGATTTCCATTGATGACAAG
GAPDH-f2	GAPDH	CCACATCGCTCAGACACCAT
GAPDH-r2	GAPDH	AAATCCGTTGACTCCGACCTT
CCND1-f1	CCND1	TGGGTCTGTGCATTTCTGGTT
CCND1-r1	CCND1	GCTGGAAACATGCCGGTTAC
CCND1-f2	CCND1	TGCGCTGCTACCGTTGACT
CCND1-r2	CCND1	AGCGATTGTAATATTTCCAAACC
Fu-f1	Fu	TGTACAAGGGTCGAAGAAAATACAGT
Fu-r1	Fu	GAGCGCCCCAATTTTGG
Fu-f2	Fu	CGCATCCTACACCGAGATATGA
Fu-r2	Fu	CAAATCCAAAGTCACAGAGCTTGA

Real Time PCR—Twenty-four hours before treatment, HeLa cells were seeded at a density of 1×10^5 cells/well of a 6-well plate. Cells were transfected with siRNAs as described. Total RNA was isolated using an RNeasy mini kit (Qiagen) following the manufacturer's instructions. cDNA was synthesized using the TaqMan reverse transcription reagents kit (Applied Biosystems), and real time PCR was carried out using the SYBRGreen PCR master mix (Applied Biosystems) according to the manufacturer's instructions with an ABI 7900HT cycler under the following conditions: 50 °C for 2 min, 95 °C for 10 min, [95 °C for 15 s, and 60 °C for 1 min] for 40 cycles and then a dissociation stage of 95 °C for 15 min, 60 °C for 15 min, and 95 °C for 15 min. Sequences of primers are listed (Table 2).

Luciferase Reporter Assay—4×10^4 HeLa cells/well of a 12-well plate were seeded 24 h prior transfection. Reporter plasmids containing eight GLI binding sites linked to firefly luciferase (1.5 μg of DNA/well) were co-transfected with GFP-GLI3 constructs (1 μg of DNA/well) and *Renilla* luciferase (1 ng of DNA/well) for normalization. Transfections with the respective plasmids were performed using JetPEI (Polyplus Transfections) according to the manufacturer's instructions. The reporter assays were carried out using the Dual-Luciferase Reporter 1000 assay system (Promega) following the manufacturer's instructions. Luciferase intensities were measured in a Centro Luminometer LB 960 (Berthold).

Immunoprecipitation—For immunoprecipitation experiments, HeLa cells were plated in 75-cm^2 flasks at a density of 8×10^5 1 day prior to transfection. Cells were transfected with the respective plasmids using JetPEI transfection reagent (Polyplus Transfections) according to the manufacturer's instructions. 48 h after transfection, the cells were lysed by sonication in IP buffer (containing 50 mM Tris, pH 7.5, 2.5 mM $MgCl_2$, 100 mM NaCl, 1 mM DTT, PhosStop (phosphatase

inhibitor mixture; Roche), complete (protease inhibitor mixture; Roche)). Immunoprecipitation was carried out using either protein G-Agarose (Roche) combined with anti-V5 (Invitrogen) or anti-HA (Covance) antibodies or anti-FLAG M2 agarose (Sigma) following the manufacturer's instructions.

Mass Spectrometry—SDS gels of immunoprecipitates were stained with Imperial Protein Stain (Pierce). The bands of interest were excised, trypsinized, and analyzed by chromatographic separation on a LC Packings 75-μm PepMap C18 column (Dionex, Idstein, Germany) using a capillary liquid chromatography CapLC system delivering a gradient to formic acid (0.1%) and acetonitrile (80%). Eluted peptides were ionized by electrospray ionization on a Q-TOF hybrid mass spectrometer (Micromass, Manchester, UK). The mass spectral data were processed into peak lists containing m/z value, charge state of the parent ion, fragment ion masses, and intensities and correlated with the SwissProt database using Mascot software (19).

Constructs—Either the full-length Fu cDNA (coding for amino acids 1–1315), Fu cDNA coding for amino acids 441–1315, or Fu cDNA coding for amino acids 1–447 was PCR-amplified on the clone IRAKp961P0834 (RZPD) and cloned either into the V5 tag multiple cloning side of pBUDCE4 (Invitrogen) using the restriction enzymes NotI and BglII or into the multiple cloning site of pTL1-HA2 (a derivative of the pSG5-vector (Stratagene), in which a SV40 early promoter and a multiple cloning site with an upstream HA epitope has been inserted, kindly provided by E. Wanker) using the restriction enzymes EcoRV and BglII. For expression in *Escherichia coli*, either the full-length Fu cDNA, or the Fu cDNA coding for amino acids 351–450 were PCR-amplified and cloned into the multiple cloning site of the pET-32a(+) vector (Novagen) using the restriction enzymes (EcoRV and HindIII for full-length Fu or SalI and NotI for amino acids 351–450). The full-length MID1-cDNA was PCR-amplified and cloned into the multiple cloning site of the vector pCMVTag2A (Stratagene) using the restriction enzymes HindIII and EcoRI. A MID1 deletion construct lacking the sequence coding for amino acids 1–196 was synthesized by usage of the QuikChange site-directed mutagenesis kit (Stratagene) following the manufacturer's instructions. The full-length ubiquitin-cDNA was PCR-amplified and cloned into the p3xFLAG-CMV10-vector (Sigma) using the restriction enzymes HindIII and BamHI. The amino acid changes K48R, K63R, and KO (all lysines mutated to arginine) were inserted into this construct by mutagenesis. HA-tagged wild type or mutant ubiquitin was cloned into the pcDNA-vector (these constructs were kindly provided by A. Trockenbacher).

Fu Expression in E. coli and Purification—N-terminal His-tagged Fu was expressed in *E. coli* BL21-CodonPlus(DE3)-RIL under standard conditions. Cell pellets were resuspended in binding buffer (50 mM sodium phosphate, pH 8.0, 300 mM NaCl, 20 mM imidazole) and lysed with a French press. The extract was centrifuged at 12,000 rpm for 30 min at 4 °C. Purification of His-Fu was carried out using nickel-nitrilotriacetic acid-agarose (Qiagen). After binding of the protein to the nickel-nitrilotriacetic acid-agarose, the column was washed with wash buffer (50 mM sodium phosphate, pH 6.0, 300 mM NaCl, 20 mM imidazole, 10% glycerol, 0.25% Tween 20) and finally eluted with imidazole. All buffers contained 20 mM imidazole for enhanced stringency, the elution buffers contained 250–500 mM imidazole and 10% glycerol for more stable solubility. All fractions were analyzed on a SDS-PAGE and finally pooled.

Fu Antibody—A Fu peptide spanning amino acids 351–450 was expressed in *E. coli* and purified as described. After dialysis of the purified peptide against PBS, the peptide was used for immunization of a rabbit (Biogenes). The Fu-specific antibodies were affinity-purified from the rabbit serum using a SulfoLink coupling gel (Pierce) column that was coated with the Fu peptide.

In Vitro Ubiquitination—HEKT cells were plated in 150-cm^2 flasks at a density of 2×10^6 1 day prior transfection. Cells were transfected with the respective plasmids using JetPEI transfection reagent (Polyplus Transfections) according to the manufacturer's instructions. 48 h after transfection cells were lysed by sonication in IP buffer (containing 50 mM Tris, 100 mM NaCl, 5 mM $MgCl_2$, 1 mM DTT, Complete (protease inhibitor mix; Roche), 0.5% Nonidet P-40). Immunoprecipitation was carried out using protein G-Agarose (Roche) and anti-HA antibodies (Covance) for HA-Fu or anti-FLAG M2 agarose (Sigma) for MID1-FLAG following the manufacturer's instructions. Peptide elution of FLAG-MID1 was done using FLAG peptides (Sigma) following the manufacturer's instructions. For *in vitro* ubiquitination, we used the ubiquitinylation kit (Biomol) following the manufacturer's instructions.

RESULTS

Fu Regulates the Subcellular Localization and Transcriptional Activity of GLI3—As we have reported previously, the MID1-α4-PP2A complex regulates the subcellular localization and transcriptional activity of GLI3 in cancer cell lines (16, 17). However, our data also suggested that this regulation indirectly involves other GLI3-interacting proteins. Because the Fu kinase promotes the nuclear localization of GLI proteins (11) and is up-regulated in cancer cells (20), we tested for a putative involvement of Fu in the regulation of GLI3 subcellular localization and activity. HeLa and U373MG cells were co-transfected with GFP-tagged GLI3 (GFP-GLI3) and either nonsilencing or three different Fu specific siRNA oligonucleotides and analyzed for GLI3 subcellular localization by light microscopy as described previously (16, 17). The transcriptional activity of GLI3 was monitored by real time PCR of the GLI3 target *cyclin D1* and in a reporter assay using a construct in which eight GLI-binding sites are fused to a luciferase gene. As shown in Fig. 1, Fu knockdown led to significant reduction of the nuclear localization of GFP-GLI3 (concomitantly, fractions of cells with cytosolic GLI3 were increased) (Fig. 1*A*) and GLI3 transcriptional activity as measured by expression of the GLI3-target cyclin D1 by real time PCR (Fig. 1*B*) and in a luciferase reporter assay (Fig. 1*C*). The efficiency of the knockdown procedure was monitored by real time PCR amplifying the endogenous Fu mRNA and by Western blot (Fig. 1*B*). In our previous studies, we have shown that the MID1 complex, similar to Fu, regulates the subcellular localization and activity of GLI3 (16, 17). Because our data also suggested that this regulation is indirect and involves another GLI3-interacting protein, we hypoth-

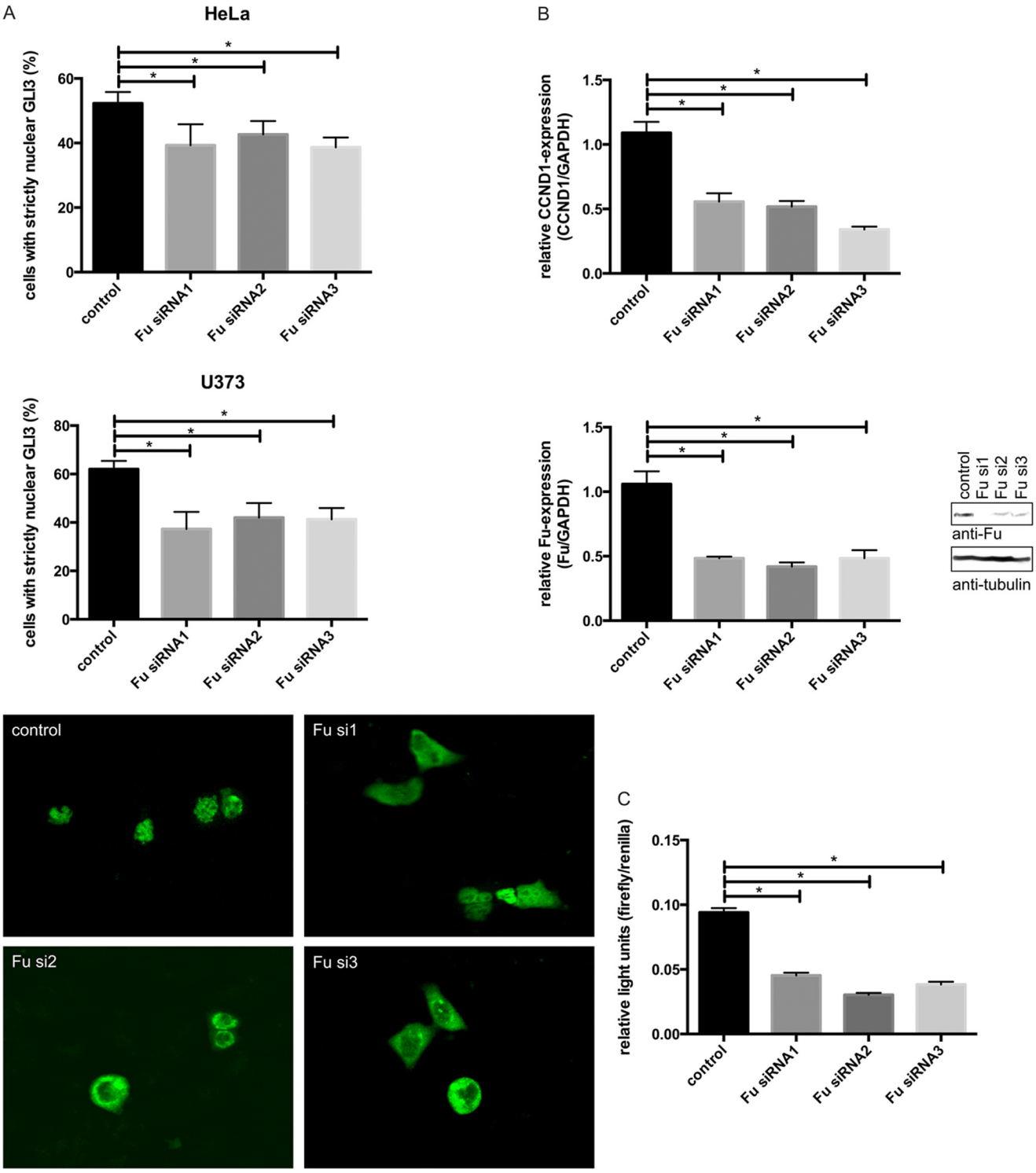

FIGURE 1. **Subcellular localization and transcriptional activity of GLI3 after Fu knockdown.** *A*, subcellular distribution of GFP-GLI3 in HeLa (*top panel*) or U373MG (*middle panel*) cells after co-transfection with either nonsilencing control siRNAs or three different Fu-specific siRNAs. GFP signal distribution in individual cells occurred in three patterns: exclusively nuclear fluorescence, even staining throughout cytosol and nucleus, or predominantly cytosolic fluorescence. Transfected cells were randomly chosen, counted, and classified in one of the three groups. The data shown represent percentages of cells showing strictly nuclear GFP-GLI3 localization (means ± S.D. scored per group from three independent experiments of 100 cells each). *, $p < 0.05$. *Bottom panel*, representative pictures of cells showing GFPGLI3 localization after transfection with nonsilencing control siRNAs or three different Fu-specific siRNAs. *B*, relative *Cyclin D1* (*upper panel*) or *Fu* (*lower panel*) mRNA amounts in HeLa cells transfected with either nonsilencing control siRNAs or three different Fu-specific siRNAs as measured by real time PCR (*lower panel, left*) and Western blot (*lower panel, right*) using Fu- or tubulin-specific antibodies. *Left*, columns represent mean values of four samples measured in parallel ± S.D. GAPDH was used for normalization. *, $p < 0.05$. *C*, GLI3 reporter assay. Firefly luciferase under the control of eight GLI-binding sites was co-transfected with three different Fu-specific siRNAs or control-siRNAs. As an internal transfection control, *Renilla* luciferase was included and used for normalization. The *columns* show relative firefly luciferase signals from four samples ± S.D. *, $p < 0.05$.

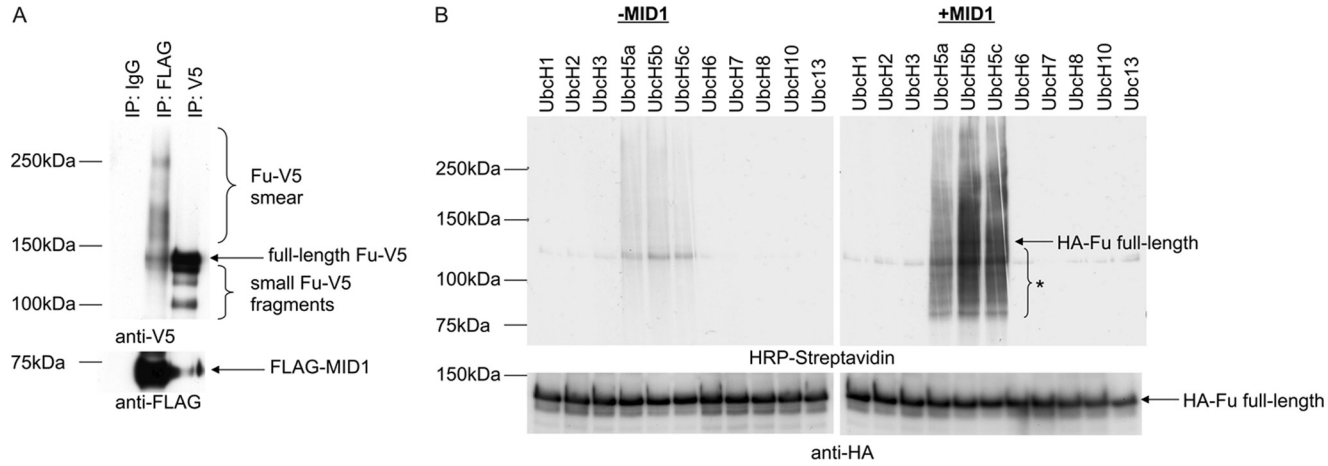

FIGURE 2. **Interaction of Fu with the ubiquitin ligase MID1.** *A*, co-immunoprecipitation of FLAG-MID1 and Fu-V5. Immunoprecipitations from HeLa cell lysates overexpressing FLAG-MID1 and Fu-V5 were performed using anti-V5 antibodies, anti-FLAG-M2-agarose, or nonspecific IgGs as negative control. Immunoprecipitates were analyzed by Western blot. FLAG-MID1 (*lower panel*) and Fu-V5 (*upper panel*) were detected using the respective antibodies. The full-length FLAG-MID1 and Fu-V5 bands, as well as shorter Fu-V5 fragments and a high molecular weight Fu-V5 smear are depicted. *B*, *in vitro* ubiquitination of HA-Fu. HA-Fu was incubated with an E1 enzyme, with a panel of 11 different E2 enzymes (UbcH1, UbcH2, UbcH3, UbcH5a, UbcH5b, UbcH5c, UbcH6, UbcH7, UbcH8, UbcH10, and Ubc13), and with (*right panels*) or without (*left panels*) the E3 enzyme MID1 and analyzed on a Western blot. The binding of biotinylated ubiquitin to HA-Fu was visualized using HRP-streptavidin (*upper panels*). To show equal loading of HA-Fu to each reaction, the same membranes were incubated with anti-HA antibodies (*lower panels*). The full-length HA-Fu bands, as well as shorter HA-Fu fragments (*asterisk*), are depicted.

esized that Fu and MID1 could interact, regulating GLI3 subcellular translocation and maturation.

Fu Interacts with the Ubiquitin Ligase MID1—To assess a putative physical interaction between Fu and the MID1 protein complex co-immunoprecipitation experiments with HeLa cell lysates overexpressing Fu-V5 and FLAG-MID1 using V5 antibodies, FLAG antibodies, and unspecific immunoglobulins as negative control were performed. Subsequently, immunoprecipitates were analyzed on Western blots. A clear co-purification of Fu-V5 and FLAG-MID1 was detected, indicating that both proteins are part of the same protein complex (Fig. 2*A*). Interestingly, in the FLAG immunoprecipitate, not only full-length Fu-V5 was co-purified, but also a high molecular weight ladder was detected, indicating post-translational modification of Fu-V5 when interacting with MID1.

Because MID1 is a ubiquitin ligase, ubiquitination was one possibility of how Fu could be post-translationally modified when complexing with MID1. This hypothesis is supported by observations of Kise and colleagues (21), who have described that Fu is ubiquitinated in mammalian cell lines. To investigate whether MID1 acts as an E3 ubiquitin ligase catalyzing the ubiquitination of Fu, *in vitro* ubiquitination assays were performed. In these assays, immunopurified FLAG-MID1 (as putative E3 enzyme) and immunopurified HA-Fu (as substrate) were incubated together with an E1 enzyme and a panel of E2 enzymes in a buffer containing biotinylated ubiquitin. Ubiquitination of Fu was visualized on Western blots using HRP-streptavidin. As negative controls, HA-Fu and E1 and E2 enzymes were incubated with FLAG immunoprecipitate obtained from HeLa cells without MID1-FLAG expression. Ubiquitination of HA-Fu could be detected with the E2 enzymes UbcH5a, UbcH5b, and UbcH5c (Fig. 2*B*). Importantly, this ubiquitination was significantly enhanced in the presence of immunopurified MID1. These data suggest that MID1 indeed has E3 ubiquitin ligase activity on Fu.

Fu Polyubiquitination Involves Lys^{6}, Lys^{48}, and Lys^{63} Linkage and Is Mediated by the MID1 Ubiquitin Ligase—Fu had previously been shown to be ubiquitinated and degraded via the proteasome (21). In confirmation of these data, we performed co-immunoprecipitation of HA-tagged Fu and FLAG-tagged ubiquitin from cells that were incubated in the presence of the proteasome inhibitor MG-132. The enrichment of polyubiquitinated Fu that was detected after incubation with the proteasome inhibitor MG-132 (Fig. 3*A*) indicates a role of the proteasome in the metabolism of ubiquitinated Fu.

Polyubiquitin chains are covalently linked via isopeptide bonds using one of seven lysines in the ubiquitin protein. The best studied polyubiquitin chains, linked via Lys^{48}, target proteins for degradation by the proteasome. However, chains can also be linked via any other of the six lysines in ubiquitin (*e.g.* Lys^{63}), as well as the N-terminal amino group of methionine. Lys^{63}-linked ubiquitin chains seem to have distinct functions, are also involved in proteasomal processes, or play a role in nonproteolytic processes like DNA repair or protein trafficking.

To analyze the nature of the ubiquitin chain *in vitro* ubiquitination assays using WT ubiquitin, ubiquitin containing only Lys^{48}, ubiquitin containing only Lys^{63}, or ubiquitin in which all Lys residues had been mutated to arginine (KO) were performed. Ubiquitination of HA-tagged Fu could be detected with WT, Lys^{63}, and Lys^{48} (Fig. 3*B*) and was significantly increased after addition of immunopurified MID1 (2.8 $\pm$ 0.5-fold increase for WT, 3.5 $\pm$ 0.5-fold increase for Lys^{63}, and 3.4 $\pm$ 0.6-fold increase for Lys^{48}). In this kind of assay, a band of monoubiquitinated Fu would be expected to appear in the KO sample if the polyubiquitin chain is added onto Fu in a stepwise manner. After long exposure times of the same blots, a very faint band was seen in the KO lane (data not shown). The reason for this very weak appearance might be either a fast turnover of monoubiquitinated into polyubiquitinated Fu. Alternatively, Fu could get ubiquitinated by

preassembled polyubiquitin chains. Some E2 enzymes are capable of preforming polyubiquitin chains on their active site cysteine, which are then transferred en bloc onto the substrate (22, 23). Taken together, these data clearly show that MID1 is able to catalyze both Lys^{48}- and Lys^{63}-linked ubiquitination of Fu *in vitro*.

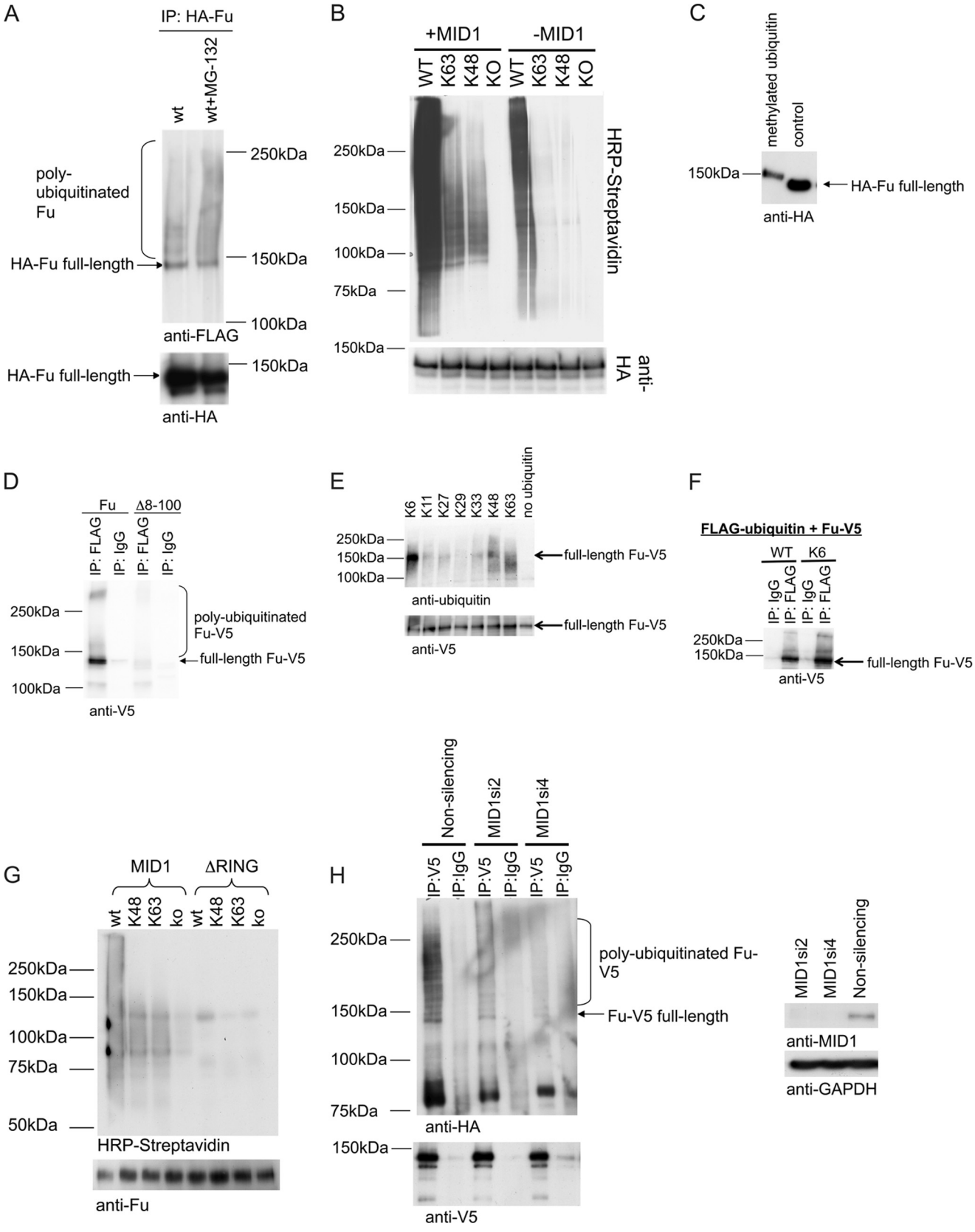

To figure out whether one mixed polyubiquitin chain or two independent polyubiquitin chains (one linked via Lys^{48} and another one linked via Lys^{63}) exist on the Fu protein, we immunopurified Fu-V5 and analyzed it by mass spectrometry. We identified only one lysine residue (Lys^{24}) to be modified by ubiquitin. However, because sequence coverage in this experiment was only ~50%, this did not rule out the existence of other ubiquitinated residues. Therefore, we performed an *in vitro* ubiquitination assay using methylated ubiquitin. Methylated ubiquitin cannot be linked into polyubiquitin chains, and therefore incorporates as a single ubiquitin-moiety, allowing the separation of molecules that are ubiquitinated on several sites by their molecular weight. *In vitro* ubiquitination of Fu with methylated ubiquitin revealed a single band at a slightly increased molecular weight, suggesting the presence of only one ubiquitination site (Fig. 3*C*). To further strengthen the hypothesis that Fu gets ubiquitinated at a single lysine residue, Lys^{24}, we used a Fu deletion construct that lacks amino acids 8–100 (Δ8–100). We performed co-immunoprecipitation of V5-tagged Fu (full-length and Δ8–100) and FLAG-tagged ubiquitin. Full-length Fu was detected in the FLAG immunoprecipitate, whereas Δ8–100 was not detectable, suggesting that this construct is ubiquitinated (Fig. 3*D*). Together, these data suggest the presence of a single polyubiquitination chain linked to Lys^{24} of Fu including both Lys^{48}- and Lys^{63}-linked ubiquitin molecules. However, these results do not preclude that this ubiquitin chain also contains ubiquitin molecules that are linked via one of the other five lysines of ubiquitin. To assess this, we have performed an *in vitro* ubiquitination assay using ubiquitin mutants in which all but one of the lysine residues have been mutated. In this experiment MID1 also catalyzed linkage with a mutant that only contained Lys^{6} (Fig. 3*E*). To verify this, we performed co-immunoprecipitation of V5-tagged Fu and FLAG-tagged WT ubiquitin, as well as ubiquitin that contained only Lys^{6}. Full-length Fu was detected in the FLAG immunoprecipitate of both WT and Lys^{6} ubiquitin (Fig. 3*F*). Taken together, our data suggest the presence of a single polyubiquitination chain linked to Lys^{24} of Fu including Lys^{6}-, Lys^{48}-, and Lys^{63}-linked ubiquitin molecules.

RING finger domains are a characteristic signature of many E3 ubiquitin ligases (24). To analyze whether the catalyzing effect of MID1 on the ubiquitination of Fu is mediated by the RING finger domain of MID1, a MID1 deletion construct lacking amino acids 1–196 was used in a similar *in vitro* ubiquitination assay as described above. In confirmation of a direct effect of the MID1-RING finger on its ubiquitin ligase activity, a clear reduction of Fu ubiquitination was detected, when immunopurified ΔRING MID1 instead of WT MID1 was added to the assay (Fig. 3*G*). Similar loading of wild type and ΔRING MID1 was controlled on Western blots (data not shown).

The previous experiments indicate that the MID1 protein is responsible for the transfer of ubiquitin onto Fu. This could be confirmed in a knockdown experiment performed in HeLa cells after co-expressing Fu-V5 and HA-ubiquitin and either nonsilencing or two different MID1 specific siRNA oligonucleotides. Fu-V5 immunoprecipitates were analyzed on a Western blot for conjugated HA-ubiquitin. Clearly, whereas in the nonsilencing control sample polyubiquitination of Fu-V5 was quite pronounced, it was significantly reduced in the MID1 knockdown samples. The efficiency of the knockdown procedure was checked on a Western blot using MID1 antibodies (Fig. 3*H*).

Fu Is a Target of Proteasome-dependent Site-specific Cleavage—Notably, both in the *in vitro* ubiquitination assays and when immunoprecipitating Fu-V5 (Fig. 2*A*, *third lane*), apart from full-length Fu-band and high molecular polyubiquitin-smear, smaller protein bands were detected. These bands could potentially refer to cleavage products of Fu. To analyze whether Fu is target of cleavage in the cell, Fu-V5 was immunopurified and put on a Coomassie-stained SDS gel. Detectable bands, several of which were congruent with the bands picked up by the anti-V5 antibody, were analyzed by mass spectrometry (Fig. 4*A* and Table 3). Fu isoforms were detected in three of the analyzed samples. Furthermore, in the 145-kDa Fu-V5 band, ubiquitin was detected, confirming ubiquitin-specific modification of Fu. A protein entity detected at ~80 kDa turned out to be a previously described interaction partner of Fu, HSP90 (21) (Fig. 4*A*, *band* marked with *asterisk*), which further confirms the specificity of the reaction.

FIGURE 3. *A*, immunoprecipitation of HA-Fu conjugated to FLAG ubiquitin. HA-Fu was co-expressed with FLAG ubiquitin with or without treatment with the proteasome inhibitor MG-132 and purified by immunoprecipitation using HA antibodies. The incorporation of ubiquitin was then detected on Western blots using FLAG antibodies (*upper panel*). To show the loading of HA-Fu to each lane, the same membranes were incubated with anti-Fu antibodies (*lower panel*). *B*, *in vitro* ubiquitination of HA-Fu. HA-Fu was incubated with an E1 enzyme, with the E2 enzyme UbcH5b, and with (+*MID1*) or without (−*MID1*) the E3 enzyme MID1 and analyzed on a Western blot. In this reaction, either WT ubiquitin or ubiquitin proteins in which all lysines have been mutated to arginine (KO), in which all lysines but Lys^{48} have been mutated to arginine (Lys^{48}), or in which all lysines but Lys^{63} have been mutated to arginine (Lys^{63}) were applied. The binding of biotinylated ubiquitin to HA-Fu was visualized using HRP-streptavidin (*upper panel*). To show equal loading of HA-Fu to each reaction, the same membranes were incubated with anti-HA antibodies (*lower panel*). *C*, *in vitro* ubiquitination of HA-Fu. HA-Fu was incubated either without or with a mixture of an E1 enzyme, the E2 enzyme UbcH5b, the E3 enzyme MID1, and methylated ubiquitin and analyzed on a Western blot. The binding of methylated ubiquitin to HA-Fu induced a shift in the molecular weight, which was detected with HA antibodies. *D*, immunoprecipitation of Fu-V5 conjugated to FLAG ubiquitin. Full-length Fu-V5 or a deletion construct lacking amino acids 8–100 (Δ8–100) was co-expressed with FLAG ubiquitin. Ubiquitinated proteins were purified by immunoprecipitation using anti-FLAG beads. Ubiquitinated Fu was then detected on Western blots using V5 antibodies. *E*, *in vitro* ubiquitination of Fu-V5. Fu-V5 was incubated either without or with a mixture of an E1 enzyme, the E2 enzyme UbcH5b, the E3 enzyme MID1, and different ubiquitin mutants in which either all (KO) or all but one lysine have been mutated. Samples were analyzed on a Western blot on which ubiquitin (*upper panel*) or Fu-V5 (*lower panel*) was detected. *F*, immunoprecipitation of Fu-V5 conjugated to FLAG ubiquitin. Full-length Fu-V5 was co-expressed with either WT FLAG ubiquitin or FLAG ubiquitin in which all lysines apart from Lys^{6} were mutated. Ubiquitinated proteins were purified by immunoprecipitation using anti-FLAG beads. Ubiquitinated Fu was then detected on Western blots using V5 antibodies. *G*, *in vitro* ubiquitination of His-Fu with an E1 enzyme, the E2 enzyme UbcH5b, and the E3 enzyme MID1 as described for Fig. 2*B*. Either full-length MID1 (*MID1*) or a MID1 deletion construct missing the first 196 amino acids (including the RING finger domain; Δ*RING*) were used. To show equal loading of His-Fu to each reaction, the same membranes were incubated with anti-Fu antibodies (*lower panel*). *H*, immunoprecipitation of Fu-V5 conjugated to HA ubiquitin. Fu-V5 and HA ubiquitin were co-transfected with either nonsilencing control siRNAs or two different MID1-specific siRNAs (*MID1si2* and *MID1si4*). *Left panel*, Fu-V5 was purified by immunoprecipitation with V5 antibodies (*IP:V5*). Pulldowns with unspecific IgGs were used as negative controls (*IP:IgG*). The immunoprecipitates were analyzed on Western blots detecting the Fu ubiquitination with anti-HA antibodies (*upper panel*). To visualize loading of Fu-V5 to each lane, the same membranes were incubated with anti-V5 antibodies (*lower panel*). *Right panel*, the efficiency of the MID1 knockdown procedure was monitored on Western blots using MID1-specific antibodies (*upper panel*) or GAPDH antibodies as loading control (*lower panel*).

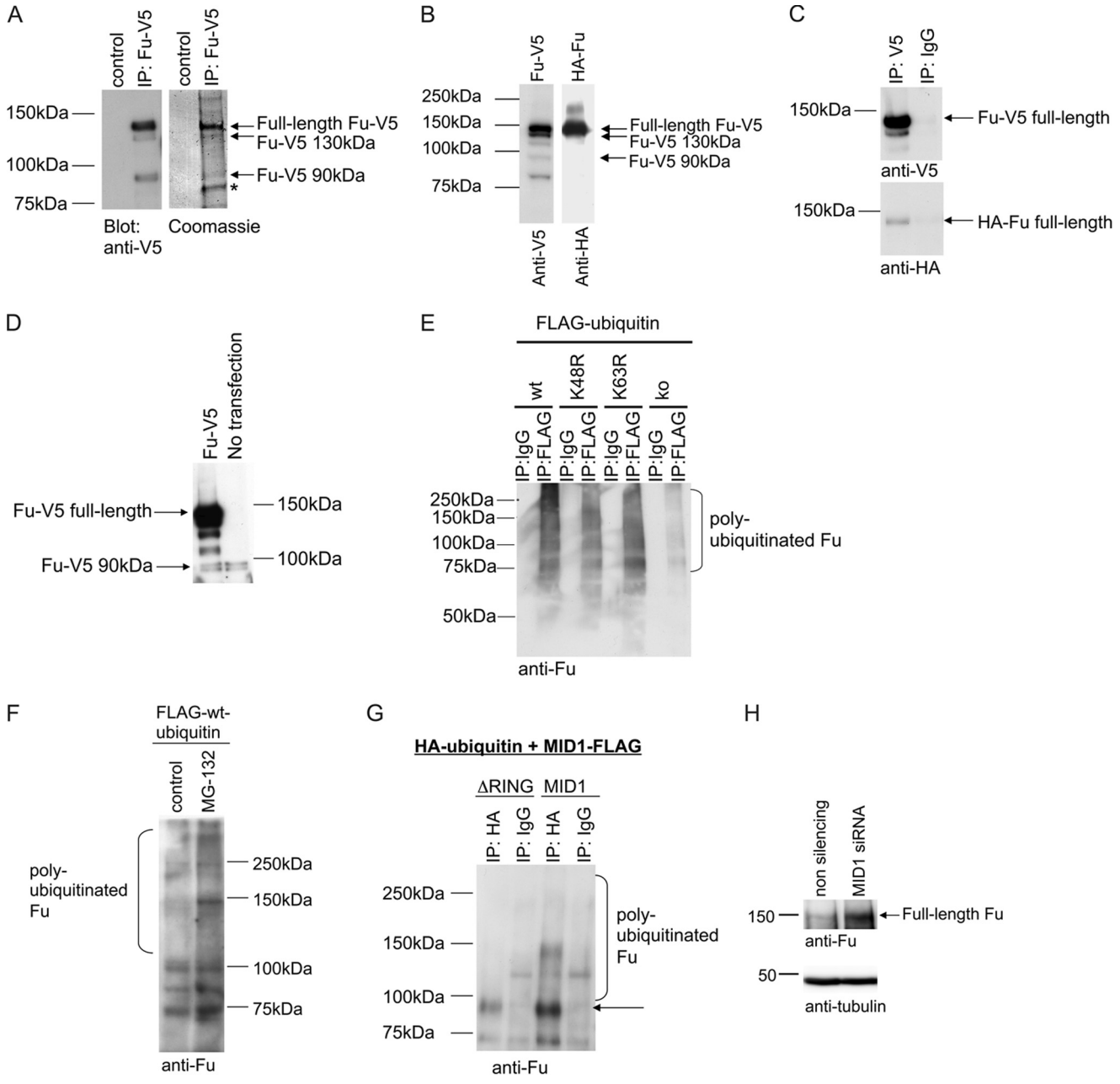

FIGURE 4. *A*, identification of different Fu isoforms by mass spectrometry. *Right panel*, immunoprecipitated Fu-V5 was separated on an SDS gel stained by Coomassie. The bands marked by *arrows* were identified as Fu isoforms by mass spectrometry; the band marked by *asterisk* was identified as Hsp90. *Left panel*, an aliquot of the same immunoprecipitate was analyzed on a Western blot using anti-V5 antibodies. *B*, detection of different Fu isoforms. Lysates of cells expressing Fu-V5 (*left panel*) or cells expressing HA-Fu (*right panel*) were analyzed on Western blot. The different Fu protein isoforms were detected with anti-V5 (*left panel*) or anti-HA (*right panel*) antibodies, respectively. *C*, homodimerization of Fu. HA-Fu and V5-Fu were co-expressed in HeLa cells and immunoprecipitated with anti-V5 antibodies or nonspecific IgGs as negative control. HA-Fu (*lower panel*) and Fu-V5 (*upper panel*) were visualized on Western blots with V5 or HA antibodies, respectively. *D*, lysates of nontransfected HeLa cells (*right lane*) or HeLa cells transfected with Fu-V5 (*left lane*) were analyzed on Western blots using the affinity-purified Fu antibody. *E*, immunoprecipitation of FLAG ubiquitin and detection of ubiquitin-coupled endogenous Fu. HeLa cells were transfected with either WT FLAG ubiquitin or ubiquitin proteins in which all lysines have been mutated to arginine (KO) or in which either Lys^{48} or Lys^{63} have been mutated to arginine (K48R or K63R). All ubiquitinated proteins from the lysates of those cells were isolated by immunoprecipitation using anti-FLAG-agarose or mouse IgG-agarose as negative control. Ubiquitinated endogenous Fu was then detected on Western blots using anti-Fu antibodies. *F*, immunoprecipitation of FLAG ubiquitin and detection of ubiquitin-coupled endogenous Fu as in *E*. Prior to immunoprecipitation, cells were incubated with or without the proteasome inhibitor MG-132. *G*, co-expression of HA ubiquitin and FLAG-MID1 wild type or FLAG-MID1 lacking amino acids 1–196 (ΔRING). Ubiquitinated proteins were purified by HA immunoprecipitation, and the relative ubiquitination of Fu was determined by Western blot analysis using Fu antibodies. *H*, stabilization of endogenous Fu after MID1 knockdown. Lysates of cells transfected with nonsilencing control siRNAs (*left lane*) or MID1-specific siRNAs (*right lane*) were analyzed on Western blot. Full-length endogenous Fu was detected with anti-Fu antibodies. Tubulin was detected on the same membranes as loading control.

Taken together, these data indicate that overexpressed Fu-V5 undergoes multiple site-specific cleavage steps, which result in at least three different isoforms of 145, 130, and 90 kDa. Because the 130- and 90-kDa Fu isoforms could only be detected when using C-terminally V5-tagged Fu but not with N-terminally tagged HA-Fu (Fig. 4*B*) and according to the

TABLE 3
Identified Fu peptides

Band 2	^{334}VAPGTAPLPR^{343}
	^{344}LGATPQESSLLAGILASELK^{363}
	^{369}SGTGEVPSAPR^{379}
	^{1251}EAALIALR^{1258}
	^{1259}SLQQEPGIHQVLVSLGASEK^{1278}
Band 3	^{125}DMKPQNILLAK^{135}
	^{141}LCDFGFAR^{148}
	^{229}DFLQGLLTK^{237}
	^{277}LPPELQVLK^{285}
	^{301}ILTQAYK^{307}
	^{318}HQNTGPALEQEDK^{330}
	^{334}VAPGTAPLPR^{343}
	^{344}LGATPQESSLLAGILASELK^{363}
	^{369}SGTGEVPSAPR^{379}
	^{369}SGTGEVPSAPR^{379}
	^{211}NVASALGNLGPEGLGEELLQCEVPQR^{1236}
	^{1251}EAALIALR^{1258}
	^{1259}SLQQEPGIHQVLVSLGASEK^{1278}
Band 4	^{25}YSAQVVALK^{33}
	^{125}DMKPQNILLAK^{135}
	^{229}DFLQGLLTK^{237}
	^{277}LPPELQVLK^{285}
	^{301}ILTQAYK^{307}
	^{318}HQNTGPALEQEDK^{330}
	^{334}VAPGTAPLPR^{343}
	^{344}LGATPQESSLLAGILASELK^{363}
	^{369}SGTGEVPSAPR^{379}
	^{390}AFPEERPEVLGQR^{402}
	^{571}LLAQPDDSEQTLR^{583}
	^{1040}LALMDPTSLNQFVNTVSASPR^{1060}
	^{1116}SLLGHPENSVR^{1126}
	^{1237}LLEMACGDPQPNVK^{1250}
	^{1251}EAALIALR^{1258}
	^{1259}SLQQEPGIHQVLVSLGASEK^{1278}

approximate molecular weights of the cleavage products, we concluded that cleavage sites are located in the N terminus of the protein cutting either within or directly C-terminal of the kinase domain. Interestingly, in the *in vitro* ubiquitination assay performed with N-terminally tagged Fu, a ubiquitination smear that migrates faster than the full-length, N-terminally tagged HA-Fu monomer was detected. One possibility to explain occurrence of these faster migrating Fu cleavage fragments could be dimerization of HA-tagged Fu and endogenous Fu in the HA immunoprecipitate. Formation of Fu dimers in the cell was proven by co-immunopurification of HA- and V5-tagged Fu (Fig. 4*C*).

Cleavage and Ubiquitination of Endogenous Fu—For the analysis of endogenous Fu, a Fu-specific polyclonal antibody directed against amino acids 351–450 was generated. Specificity of the antibody was established in several different assays: (i) Fu was detected in lysates of either nontransfected HeLa cells or HeLa cells overexpressing Fu-V5. In Fu-V5-expressing HeLa cell lysates, the Fu antibody specifically detected the previously characterized bands corresponding to Fu-V5 in transfected cells. Among those were bands at a molecular mass of ~90 kDa. In nontransfected cells, however, although bands of 90 kDa were picked up, full-length Fu was not detected (Fig. 4*D*). (ii) Preincubation of the antibody with *E. coli* expressed and purified full-length Fu blocked off detection of only the 90-kDa signal (data not shown), indicating specificity of this band. (iii) Finally, specificity of the 90-kDa band was further confirmed in a knockdown approach in which the signal was significantly reduced after Fu-specific knockdown compared with the nonsilencing control sample (Fig. 1). Taken together, these data show that the produced antibody detects a cleaved isoform of Fu in a set of different (cancer) cell lines, which seems to be the predominant Fu isoform in these cell lines.

The established Fu antibody was then used to assess ubiquitination of endogenous Fu. HeLa cells were transfected with FLAG-tagged ubiquitin (either WT, K63R, K48R, or KO). Ubiquitinated proteins were immunoprecipitated using an anti-FLAG antibody, and immunoprecipitates were analyzed on a Western blot for the presence of endogenous Fu. In confirmation of the results we had obtained with HA-Fu, a significant number of ubiquitinated Fu species were detected. Expression of K48R or K63R ubiquitin mutants instead of WT ubiquitin still allowed Fu ubiquitination (Fig. 4*E*). Application of the proteasome inhibitor MG132 prior to immunoprecipitation led to an accumulation of (monoubiquitinated) full-length Fu (145 kDa) (Fig. 4*F*), which strongly suggests that the cleavage of Fu into its shorter protein isoform is mediated by the proteasome.

Furthermore, MID1 dependence of Fu ubiquitination/cleavage was demonstrated by overexpression of wild type MID1 in comparison to the inactive RING finger deletion construct in HeLa cells. Immunoprecipitation of HA-tagged ubiquitin and subsequent Western blot analysis of the immunoprecipitates with the anti-Fu antibody led to an increase of both polyubiquitinated Fu forms, as well as the expression of the cleaved 90-kDa fragment (Fig. 4*G*). These data suggest that the MID1 ubiquitin ligase promotes both ubiquitin-dependent modification and cleavage of endogenous Fu. In line with this, MID1 knockdown led to stabilization of endogenous full-length Fu (Fig. 4*H*).

N-terminally cleaved Fu promotes GLI3 nuclear localization and transcriptional activity—The final question we asked was whether the cleaved C-terminal Fu fragment is active in meditating the nuclear translocation and activation of the GLI3 transcription factor. To answer this question, we cloned a Fu deletion construct lacking amino acids 1–440 (which includes the Fu kinase domain) to mimic the 90-kDa Fu C-terminal cleavage product (ΔN-term). This construct, as well as a corresponding constructs containing only the isolated kinase domain of Fu or the full-length Fu, was used to analyze effects on the subcellular localization of GLI3. Interestingly, the ΔN-term construct was able to increase the nuclear localization of GLI3 similarly to wild type Fu, whereas co-expression of the isolated kinase domain did not induce such an effect (Fig. 5*A*). In line with this, the transcriptional activity of GLI3 also increased significantly after co-expression of full-length Fu, as well as the ΔN-term Fu construct (Fig. 5*B*). By contrast, inhibiting Fu cleavage by blocking the proteasome with *N*-acetyl-L-leucinyl-L-leucinal-L-norleucinal (LLnL) led to the opposite effect. GLI3 nuclear translocation is inhibited after such treatment (Fig. 5*C*). This means that for GLI3 translocation, the kinase domain Fu is dispensable and that the cleaved product that we see in the different tumor cells is responsible for translocating GLI3 to the nucleus and for activating GLI3.

Taken together, these results show that, mediated by a protein-protein interaction between Fu and the ubiquitin ligase MID1, a mixed Lys6/Lys^{48}/Lys^{63} ubiquitin chain is added onto Fu. This ubiquitin modification mediates proteasomal cleavage of the molecule, producing a C-terminal Fu fragment that lacks the N-terminal kinase domain. The C-terminal fragment rather

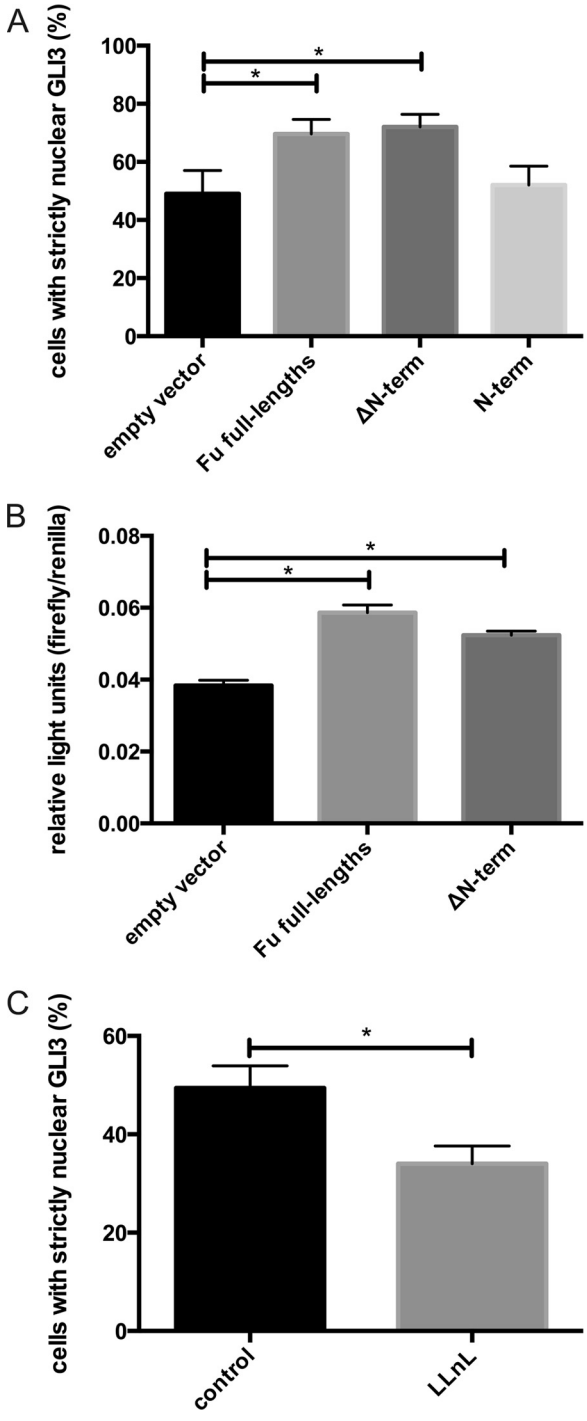

FIGURE 5. **Subcellular localization and transcriptional activity of GLI3 after Fu-overexpression.** *A*, subcellular distribution of GFP-GLI3 in HeLa cells after co-transfection with either empty vector (*left columns*), full-length Fu, a Fu construct lacking the N-terminal kinase domain (ΔN-term), or a construct containing the isolated Fu kinase domain (*N-term*, *right columns*). GFP-GLI3 signal distribution was quantified as described for Fig. 1*A*. Means ± S.D. scored per group from three independent experiments of 100 cells each are shown. *, $p < 0.05$. *B*, GLI3 reporter assay. Firefly luciferase under the control of eight GLI-binding sites was co-transfected with empty vector (*left column*), full-length Fu (*middle column*), or ΔN-term (*right column*). As an internal transfection control, *Renilla* luciferase was included and used for normalization. Columns show relative firefly luciferase signals from four samples ± S.D. *, $p < 0.05$. *C*, subcellular distribution of GFP-GLI3 in HeLa cells that were treated with or without the proteasome inhibitor *N*-acetyl-L-leucinyl-L-leucinal-L-norleucinal (*LLnL*). The data were analyzed and are presented as described for Fig. 1*A*. Means ± S.D. scored per group from three independent experiments of 100 cells each are shown. *, $p < 0.05$.

than the full-length molecule seems to play the active part in mediating the nuclear translocation and maturation of GLI3 into an active transcriptional regulator. Our data provide a cellular function for Fu, a regulatory mechanism underlying the subcellular transposition of the transcriptional activator GLI3 that links the MID1 ubiquitin ligase with GLI3, Fu, and SHH signaling.

DISCUSSION

Fu is an essential component of Hh signaling in *Drosophila*, but the biochemical functions of mammalian Fu remain as yet unclear. Here, we show that human Fu controls the subcellular localization and transcriptional activity of GLI3 in cancer cell lines. Furthermore, we found that the MID1 protein complex, which we have previously shown to regulate GLI3 signaling (16, 17), interacts with Fu and catalyzes its ubiquitin-dependent modification and site-specific cleavage. A ΔN-term fragment is produced by the proteasome upon MID1-dependent ubiquitination that is capable of regulating GLI3, suggesting a kinase domain-independent mode of action of Fu on GLI3.

Fu Regulates GLI3 Signaling—The role of mammalian Fu in GLI regulation has been discussed controversially. Although some studies suggest that Fu is dispensable for the regulation of GLIs, because it has little or no effect on GLI activities (12), others have shown that human Fu binds to GLI1, GLI2, and GLI3 and promotes nuclear localization of GLI1 and GLI2 (11). Furthermore, human Fu was shown to enhance reporter activities of GLI1 and GLI2 (21). We show here that depletion of Fu leads to cytosolic retention and decreased transcriptional activity of the transcription factor GLI3, an effector molecule of SHH signaling. An explanation for these contradictory results could be tissue/cell specificity of the function(s) of Fu. In this study, we have used human cancer cell lines (HeLa and U373MG), in which autonomously activated SHH signaling was observed (16). In these cell lines, the subcellular localization and activity of GLIs might be regulated differently from cell lines without autonomously activated SHH signaling.

Fu Ubiquitination—Polyubiquitination and proteasomal degradation of Fu have been demonstrated previously (21). In confirmation of these data, we show here polyubiquitination of Fu, which increases after proteasomal inhibition. Although theoretically all seven lysines of ubiquitin can contribute to the assembly of ubiquitin molecules and a variety of polyubiquitin chains of diverse length and linkages can be produced (25, 26), canonical Lys^{48}-linked ubiquitin chains seem to be the principal signal for proteasomal degradation. By contrast, Lys^{63}-linked chains were long believed to primarily play a role in non-proteolytic processes of protein function regulation in, for example, DNA repair or protein trafficking. Only recently, Lys^{63} ubiquitin chains have also been linked to proteasomal cleavage and degradation (reviewed in Ref. 27). We have identified polyubiquitination of Fu involving both Lys^{48} and Lys^{63} linkage. The presence of mixed polyubiquitin chains has been suggested earlier. Although experiments by Xu *et al.* (28) have shown that only non-Lys^{63}-linked chains are involved in proteasomal degradation, other studies have provided evidence for polyubiquitin chains with Lys^{63} linkages to also be involved in degradation processes. Thus, mixed polyubiquitin chains with

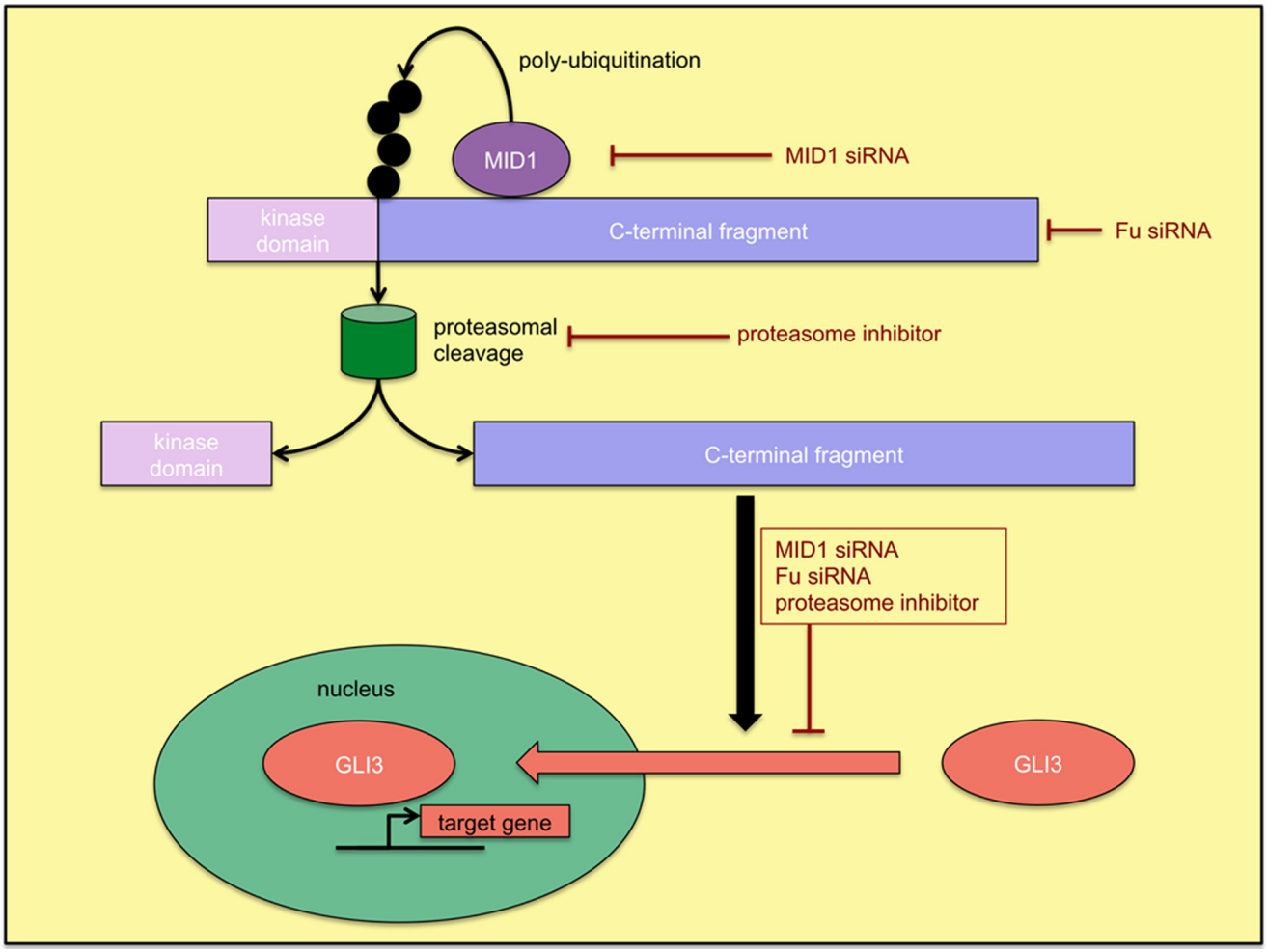

FIGURE 6. **Hypothetical model.** MID1 catalyzes the ubiquitination of Fu, thereby promoting proteasomal cleavage of Fu. The C-terminal fragment of Fu promotes nuclear localization of GLI3 and activates its target genes. Like MID1 and Fu knockdown, the inhibition of the proteasome leads to cytosolic retention of GLI3.

Lys^{11}, Lys^{48}, and Lys^{63} linkages are competent to mediate cyclinB1 degradation (29), and Lys^{63} chains were reported to accumulate after proteasomal inhibition (30, 31). The latter has been confirmed in this study. The Fu protein not only seems to be modified with ubiquitin molecules linked via Lys^{6}, Lys^{48}, and Lys^{63}, but also these types of linkage appear to be connected with proteasomal degradation and site-specific cleavage of Fu. However, our data do not exclude the existence of linkage via the N-terminal amino group of methionine, because we have only tested linkage via different lysine residues in this study.

Fu Is a Target of Site-specific Cleavage by the Proteasome—We show here that the Fu protein is cleaved into shorter protein fragments. Cleavage events regulating the activity of proteins of the SHH pathway have been described for SHH or GLI3 as well. Although cleavage of full-length SHH is necessary to form the active SHH-ligand (3), which then binds its receptor PTC1, GLI3 cleavage into its repressor form takes place in the absence of a SHH signal (32). We show here that ubiquitination of Fu mediates its proteasomal cleavage, forming a fragment that lacks the N-terminal serine/threonine kinase domain. Furthermore, we provide evidence that this ΔN-term fragment rather than the isolated kinase domain or the full-length protein plays the active part in the regulation of the subcellular translocation of GLI3. This separates the GLI3 regulatory function of Fu from its kinase activity, supporting previous reports that also have suggested the existence of kinase domain-independent functions of Fu by using kinase-inactive Fu mutants (33).

ΔN-term Fu Fragment: A Key in the Up-regulation of SHH in Cancer?—Interestingly, the cleaved Fu fragment represents the major endogenous protein isoform in all cancer cell lines we have analyzed in this study. This raises the question of whether Fu cleavage is a process that is enhanced in cancer cells. Kise *et al.* (21) showed Western blots of endogenous full-length Fu in COS7, HEK293, and PC3 cells; however the antibody used in this study (detecting amino acids 1–304) most probably would not be suitable to detect the C-terminal fragments that we detected with our antibody (detecting amino acids 351–450). This leaves open the question of whether cleaved Fu isoforms also exist in cell types other than those we have analyzed here. In the future, it will be interesting to see whether the predominant existence of the ΔN-term Fu fragment is characteristic for cancer cells with autonomously activated SHH as has been shown for the cell lines used in this study. Autonomous SHH activation has been demonstrated to be an important growth-stimulating factor in diverse cancers (34–37). Dysregulation of Fu cleavage leading to an overproduction of the ΔN-term Fu

fragment and an autonomous translocation and activation of GLI3 would be a plausible mechanism to explain SHH overactivation in cancer cells. Accordingly inhibition of Fu cleavage could be a promising new target in cancer cells with autonomous SHH signaling.

MID1 Catalyzes Fu Ubiquitination—MID1 is a RING finger protein, which has been shown to act as an E3 ubiquitin ligase, targeting PP2A for proteasomal degradation (18), suggesting a catalyzing effect of MID1 on Lys^{48}-linked ubiquitin chains. In a paper published by Han *et al.* (38), Lys^{63}-linked autoubiquitination of MID1 mediated through its own RING finger has been demonstrated. In this study, we have identified Fu as a novel target of the ubiquitin ligase MID1. We show that MID1 not only catalyzes Fu ubiquitination of Lys^{48}-linked but also of Lys^{6}- and Lys^{63}-linked chains. Furthermore, we found that the E2 enzymes UbcH5a, UbcH5b, and UbcH5c, together with the E3 enzyme MID1, ubiquitinate Fu most efficiently. This observation is in line with data from Napolitano *et al.* (39), who observed that MID1 interacts, among others, with UBCH5a, UBCH5b, and UBCH5c in a yeast two-hybrid assay. Another example of a RING finger protein that can catalyze linkages via several lysine residues is MuRF1. MuRF1 was shown to catalyze different kinds of polyubiquitination events on its substrate troponin I: (i) Together with the E2 enzyme UbcH1, MuRF1 catalyzes the linkage of both pure Lys^{48}- or Lys^{63}-linked chains, which target the substrate for proteasomal degradation *in vitro*. (ii) Together with the E2 enzyme UbcH5 MuRF1 catalyzes the linkage of a mixed forked chain, which includes Lys^{48}, Lys^{63}, and other linkages. However, these mixed forked chains have little capacity to target the substrate for proteasomal degradation (40). Based on the observation that the corresponding E2 enzyme might control the type of the ubiquitin tail that is catalyzed by the RING finger protein, we think that MID1 together with UbcH5 catalyzes a mixed forked chain on the Fu protein, which mediates proteasome-dependent cleavage of the molecule into a ΔN-term Fu fragment. This fragment then carries out Fu functions independently of its kinase domain. However, because in all our *in vitro* ubiquitination assays, immunopurified MID1 was used, it cannot be fully excluded that the E3 ubiquitin ligase activity that promoted Fu ubiquitination was provided by a so far uncharacterized co-factor being tightly associated to the RING finger domain of MID1 that was not removed during immunopurification.

In summary, we have shown here that Fu is involved in the activation of SHH/GLI3 signaling in cancer cell lines. However, Fu knock-out mice do not show phenotypes that correlate with dysfunctional GLI3 signaling (14, 15). One explanation for this discrepancy is that GLI3 signaling is differently regulated depending on the cellular background: although Fu is dispensable for GLI3 regulation during embryogenesis, it becomes an important regulator in adult, tumorogenic tissue. In cancer tissue, the cleaved GLI3-activating ΔN-term fragment seems to be the most abundant isoform of Fu. Because both GLI3 activity and the ubiquitination of Fu are regulated by the MID1-complex, it is likely that the MID1-dependent regulation of GLI3 is indirect and mediated by the interaction between Fu and MID1 (Fig. 6). In this scenario, MID1 catalyzes the ubiquitination of Fu, thereby promoting the production of the cleaved isoform. The ΔN-term isoform is necessary to promote formation of the full-length GLI3 activator, which translocates to the nucleus and activates its target genes. This is supported by the observation that all three, MID1 knockdown, Fu knockdown, and inhibition of proteasomal cleavage of Fu, lead to similar effects, which are the cytosolic retention and deactivation of GLI3. Because our data were collected in cancer cell lines, it is plausible to believe that the "overproduction" of cleaved Fu and the thereby induced "overactivity" of GLI3 might contribute to cancerogenesis and support tumor development, making the ΔN-term Fu isoform an interesting new cancer target.

Acknowledgments—We thank Meike Brömer and Dan Ehninger for critical reading of the paper.

REFERENCES

1. Nybakken, K., and Perrimon, N. (2002) Hedgehog signal transduction: recent findings. *Curr. Opin. Genet. Dev.* **12,** 503–511
2. Ingham, P. W., and McMahon, A. P. (2001) Hedgehog signaling in animal development: paradigms and principles. *Genes Dev.* **15,** 3059–3087
3. Villavicencio, E. H., Walterhouse, D. O., and Iannaccone, P. M. (2000) The sonic hedgehog-patched-gli pathway in human development and disease. *Am. J. Hum. Genet.* **67,** 1047–1054
4. Murone, M., Rosenthal, A., and de Sauvage, F. J. (1999) Hedgehog signal transduction: from flies to vertebrates. *Exp. Cell Res.* **253,** 25–33
5. Nybakken, K. E., Turck, C. W., Robbins, D. J., and Bishop, J. M. (2002) Hedgehog-stimulated phosphorylation of the kinesin-related protein Costal2 is mediated by the serine/threonine kinase fused. *J. Biol. Chem.* **277,** 24638–24647
6. Therond, P. P., Knight, J. D., Kornberg, T. B., and Bishop, J. M. (1996) Phosphorylation of the fused protein kinase in response to signaling from hedgehog. *Proc. Natl. Acad. Sci. U.S.A.* **93,** 4224–4228
7. Hammerschmidt, M., Brook, A., and McMahon, A. P. (1997) The world according to hedgehog. *Trends Genet.* **13,** 14–21
8. Carpenter, D., Stone, D. M., Brush, J., Ryan, A., Armanini, M., Frantz, G., Rosenthal, A., and de Sauvage, F. J. (1998) Characterization of two patched receptors for the vertebrate hedgehog protein family. *Proc. Natl. Acad. Sci. U.S.A.* **95,** 13630–13634
9. Hui, C. C., Slusarski, D., Platt, K. A., Holmgren, R., and Joyner, A. L. (1994) Expression of three mouse homologs of the Drosophila segment polarity gene cubitus interruptus, Gli, Gli-2, and Gli-3, in ectoderm- and mesoderm-derived tissues suggests multiple roles during postimplantation development. *Developmental biology* **162,** 402–413
10. Ruppert, J. M., Vogelstein, B., Arheden, K., and Kinzler, K. W. (1990) GLI3 encodes a 190-kilodalton protein with multiple regions of GLI similarity. *Mol. Cell Biol.* **10,** 5408–5415
11. Murone, M., Luoh, S. M., Stone, D., Li, W., Gurney, A., Armanini, M., Grey, C., Rosenthal, A., and de Sauvage, F. J. (2000) Gli regulation by the opposing activities of fused and suppressor of fused. *Nature cell biology* **2,** 310–312
12. Osterlund, T., Everman, D. B., Betz, R. C., Mosca, M., Nothen, M. M., Schwartz, C. E., Zaphiropoulos, P. G., and Toftgard, R. (2004) The FU gene and its possible protein isoforms. *BMC Genomics* **5,** 49
13. Daoud, F., and Blanchet-Tournier, M. F. (2005) Expression of the human FUSED protein in Drosophila. *Dev. Genes Evol.* **215,** 230–237
14. Merchant, M., Evangelista, M., Luoh, S. M., Frantz, G. D., Chalasani, S., Carano, R. A., van Hoy, M., Ramirez, J., Ogasawara, A. K., McFarland, L. M., Filvaroff, E. H., French, D. M., and de Sauvage, F. J. (2005) Loss of the serine/threonine kinase fused results in postnatal growth defects and lethality due to progressive hydrocephalus. *Mol. Cell Biol.* **25,** 7054–7068
15. Chen, M. H., Gao, N., Kawakami, T., and Chuang, P. T. (2005) Mice deficient in the fused homolog do not exhibit phenotypes indicative of perturbed hedgehog signaling during embryonic development. *Mol. Cell Biol.* **25,** 7042–7053

16. Krauss, S., Foerster, J., Schneider, R., and Schweiger, S. (2008) Protein phosphatase 2A and rapamycin regulate the nuclear localization and activity of the transcription factor GLI3. *Cancer Res.* **68,** 4658–4665
17. Krauss, S., So, J., Hambrock, M., Kohler, A., Kunath, M., Scharff, C., Wessling, M., Grzeschik, K. H., Schneider, R., and Schweiger, S. (2009) Point mutations in GLI3 lead to misregulation of its subcellular localization. *PLoS ONE* **4,** e7471
18. Trockenbacher, A., Suckow, V., Foerster, J., Winter, J., Krauss, S., Ropers, H. H., Schneider, R., and Schweiger, S. (2001) MID1, mutated in Opitz syndrome, encodes an ubiquitin ligase that targets phosphatase 2A for degradation. *Nat. Genet.* **29,** 287–294
19. Perkins, D. N., Pappin, D. J., Creasy, D. M., and Cottrell, J. S. (1999) Probability-based protein identification by searching sequence databases using mass spectrometry data. *Electrophoresis* **20,** 3551–3567
20. Dierks, C., Grbic, J., Zirlik, K., Beigi, R., Englund, N. P., Guo, G. R., Veelken, H., Engelhardt, M., Mertelsmann, R., Kelleher, J. F., Schultz, P., and Warmuth, M. (2007) Essential role of stromally induced hedgehog signaling in B-cell malignancies. *Nature medicine* **13,** 944–951
21. Kise, Y., Takenaka, K., Tezuka, T., Yamamoto, T., and Miki, H. (2006) Fused kinase is stabilized by Cdc37/Hsp90 and enhances Gli protein levels. *Biochem. Biophys. Res. Commun.* **351,** 78–84
22. Li, W., Tu, D., Brunger, A. T., and Ye, Y. (2007) A ubiquitin ligase transfers preformed polyubiquitin chains from a conjugating enzyme to a substrate. *Nature* **446,** 333–337
23. Ravid, T., and Hochstrasser, M. (2007) Autoregulation of an E2 enzyme by ubiquitin-chain assembly on its catalytic residue. *Nature cell biology* **9,** 422–427
24. Meroni, G., and Diez-Roux, G. (2005) TRIM/RBCC, a novel class of 'single protein RING finger' E3 ubiquitin ligases. *BioEssays: news and reviews in molecular, cellular and developmental biology* **27,** 1147–1157
25. Li, W., and Ye, Y. (2008) Polyubiquitin chains: functions, structures, and mechanisms. *Cellular and molecular life sciences: CMLS* **65,** 2397–2406
26. Pickart, C. M., and Fushman, D. (2004) Polyubiquitin chains: polymeric protein signals. *Current opinion in chemical biology* **8,** 610–616
27. Kravtsova-Ivantsiv, Y., Sommer, T., and Ciechanover, A. (2013) The lysine48-based polyubiquitin chain proteasomal signal: not a single child anymore. *Angewandte Chemie* **52,** 192–198
28. Xu, P., Duong, D. M., Seyfried, N. T., Cheng, D., Xie, Y., Robert, J., Rush, J., Hochstrasser, M., Finley, D., and Peng, J. (2009) Quantitative proteomics reveals the function of unconventional ubiquitin chains in proteasomal degradation. *Cell* **137,** 133–145
29. Kirkpatrick, D. S., Hathaway, N. A., Hanna, J., Elsasser, S., Rush, J., Finley, D., King, R. W., and Gygi, S. P. (2006) Quantitative analysis of in vitro ubiquitinated cyclin B1 reveals complex chain topology. *Nature cell biology* **8,** 700–710
30. Bennett, E. J., Shaler, T. A., Woodman, B., Ryu, K. Y., Zaitseva, T. S., Becker, C. H., Bates, G. P., Schulman, H., and Kopito, R. R. (2007) Global changes to the ubiquitin system in Huntington's disease. *Nature* **448,** 704–708
31. Meierhofer, D., Wang, X., Huang, L., and Kaiser, P. (2008) Quantitative analysis of global ubiquitination in HeLa cells by mass spectrometry. *Journal of proteome research* **7,** 4566–4576
32. Jacob, J., and Briscoe, J. (2003) Gli proteins and the control of spinal-cord patterning. *EMBO Rep.* **4,** 761–765
33. Maloveryan, A., Finta, C., Osterlund, T., and Kogerman, P. (2007) A possible role of mouse Fused (STK36) in Hedgehog signaling and Gli transcription factor regulation. *Journal of cell communication and signaling* **1,** 165–173
34. Berman, D. M., Karhadkar, S. S., Maitra, A., Montes De Oca, R., Gerstenblith, M. R., Briggs, K., Parker, A. R., Shimada, Y., Eshleman, J. R., Watkins, D. N., and Beachy, P. A. (2003) Widespread requirement for Hedgehog ligand stimulation in growth of digestive tract tumours. *Nature* **425,** 846–851
35. Watkins, D. N., Berman, D. M., Burkholder, S. G., Wang, B., Beachy, P. A., and Baylin, S. B. (2003) Hedgehog signalling within airway epithelial progenitors and in small-cell lung cancer. *Nature* **422,** 313–317
36. Thayer, S. P., di Magliano, M. P., Heiser, P. W., Nielsen, C. M., Roberts, D. J., Lauwers, G. Y., Qi, Y. P., Gysin, S., Fernandez-del Castillo, C., Yajnik, V., Antoniu, B., McMahon, M., Warshaw, A. L., and Hebrok, M. (2003) Hedgehog is an early and late mediator of pancreatic cancer tumorigenesis. *Nature* **425,** 851–856
37. Sanchez, P., Hernandez, A. M., Stecca, B., Kahler, A. J., DeGueme, A. M., Barrett, A., Beyna, M., Datta, M. W., Datta, S., and Ruiz i Altaba, A. (2004) Inhibition of prostate cancer proliferation by interference with SONIC HEDGEHOG-GLI1 signaling. *Proc. Natl. Acad. Sci. U.S.A.* **101,** 12561–12566
38. Han, X., Du, H., and Massiah, M. A. (2011) Detection and characterization of the in vitro e3 ligase activity of the human MID1 protein. *Journal of molecular biology* **407,** 505–520
39. Napolitano, L. M., Jaffray, E. G., Hay, R. T., and Meroni, G. (2011) Functional interactions between ubiquitin E2 enzymes and TRIM proteins. *The Biochemical journal* **434,** 309–319
40. Kim, Y. S., Kang, H. S., and Jetten, A. M. (2007) The Kruppel-like zinc finger protein Glis2 functions as a negative modulator of the Wnt/beta-catenin signaling pathway. *FEBS Lett.* **581,** 858–864